Diagnosing the meteorological conditions associated with sprites and lightning with large Change Moment Charges (CMC) over Oklahoma

Lizxandra Flores Rivera[1] and Timothy Lang[2]

[1]*Department of Physics, University of Puerto Rico at Mayagüez*
[2]*NASA Marshall Space Flight Center*

Abstract

Sprites are a category of Transient Luminous Events (TLE's) that occur in the upper atmosphere above the tops of Mesoscale Convective Systems (MCSs). They are commonly associated with lightning strokes that produce large charge moment changes (CMCs). Synergistic use of satellite and radar-retrieved observations together with sounding data, forecasts, and lightning-detection-networks allowed the diagnosis and analysis of the meteorological conditions associated with sprites as well as large-CMC lightning over Oklahoma.

I. Introduction

Thunderstorms are precipitating cloud systems that also produce lightning. Thunderstorms drive the global circuit due to the separation, transfer, and neutralization of charges within the storms. The electrical structure of thunderclouds suggests that collisions between graupel, hailstones, and ice crystals in the presence of super cooled liquid water droplets, coupled with differential sedimentation rates of hydrometeors, produce charge separation and subsequent lightning.

The exact mechanisms for this type of charging are not completely understood. Some studies have shown that magnitude and sign of charge transfer are dependent on temperature (Takahashi 1978), liquid water (Takahashi 1978) or equivalent liquid water content (Saunders et. al. 1991, Saunders and Brooks 1992), size of ice crystals, impact velocity and contaminants within the hydrometeors (Jayaratne et. al. 1983, Keith and Saunders 1990). However, significant non-inductive charging occurs only when large particles are riming (i.e., when precipitation-sized ice fall through a cloud and collides with super-cooled droplets, the liquid water freezes onto them).

There are two principal types of lightning: Intracloud or cloud-to-cloud (IC) and Cloud-to-Ground (CG). In a CG stroke, a stepped leader from the cloud ionizes the column of air as the leader moves downward, and when the stepped leader reached the ground return stroke neutralizes the cloud charges. The entire multi-stroke process is collectively termed a flash (Lyons 2006).

Transient Luminous events (TLEs) are optical phenomena that occur in the upper atmosphere. Sprites, one of the most common types of TLE, often are related to lightning strokes within

Mesoscale Convective Systems (MCSs). A sprite is characterized by its red color, and occurs primarily due to dielectric breakdown in the mesosphere (80-90km).

Most of the weather experienced day-to-day is associated with the mesoscale, systems with scale lengths of tens to hundreds of kilometers (Ray 1986, Fujita 1992). MCSs produce a significant fraction of the warm-season rainfall, lightning, and severe weather in the central United States (e.g., Fritsch et. al. 1986, Goodman and MacGorman 1986, Houze et. al. 1990). In this paper we will examine the meteorological conditions associated with the location of large-CMC and sprite-parent lightning relative to storm structure. Our specific goal is to develop diagnostics to identify storms which contains sprites. NASA really want to know what kind of interference do sprites makes to aerospace activities in the 20-100km layer.

II. Methodology

- Overview

We examine case studies of TLE-producing storms using data from weather radar, satellite, radiosondes, and lightning-detection networks. Understanding these meteorological conditions is important. Studies have shown a clear link between the weather in Earth's troposphere and the electrodynamic behavior of the mesosphere (between 50 and 80 km altitude) and ionosphere (between 80 km and up; Cummer and Inan 1997).

- Radar and satellite imagery

The radar and satellite imagery were obtained from the http://www.mmm.ucar.edu/imagearchive/ website. This website is maintained by the Mesoscale and Microscale Meteorology (MMM) division of the National Center for Atmospheric Research (NCAR). The spatial domain is largely limited to the central United States. A large portion of the archive originates from within NCAR, and other images are simply downloaded from other sources such as the National Oceanic and Atmospheric Administration (NOAA). All images collected in this research were chosen to isolate and identify case-study periods.

- Sounding data

Atmospheric sounding data, provided by University of Wyoming, were taken from the closest site. Parameters include:

a) Relative humidity (RH) - One way to identify moisture in the atmosphere is calculating the RH. It is the ratio of the amount of water vapor in a given volume of air to the amount that volume would hold if the air were saturated. The formula is given by $100\% \times \frac{w}{w_s}$, where w is the mixing ratio and w_s is the saturated mixing ratio.
b) Lifting Condensation Level (LCL) - LCL is defined as the level in which an unsaturated, but moist, parcel of air can be lifted adiabatically before it becomes saturated with respect to a liquid water surface.

If a material undergoes a change in it is physical state (i.e., volume, pressure, temperature) without adding or withdrawing any heat the change is said to be adiabatic. The term Dry

Adiabatic refers to when air parcel rises in the atmosphere without becoming saturated and its temperature decreases with altitude. Intercepting 1000 hPa, dry adiabatic lines runs diagonally upward from right to left (Fig. 2). Dry adiabatic is also called lines of potential temperature; its values are labeled from 0 ºC to 80 ºC and it is represented by curved brown lines in Fig. 2.

If the water vapor is condensed inside the air parcel (which means that is releasing heat latent due to further adiabatic lifting then the process is called Saturated Adiabatic. These curves show a different rate of decrease temperature with height. They are curved solid green lines (Fig. 2) that go upward until they become parallel to the dry adiabat, due to the lack of water vapor high up in the atmosphere. Other sounding parameters include:

c) Convective Condensation Level (CCL) - If the surface temperature becomes hot enough, due to thermal convection, the surface air parcel can rise adiabatically until it condenses. This level is called the CCL.
d) Level of Free Convection (LFC) - The LFC is the level at which the parcel of air is saturated and any moist adiabatic lift thereafter would cause the parcel to become warmer and less dense than the surrounding air, thereby leading to buoyant ascent.

Meteorologists can determine the stability of the atmosphere by calculating the lapse rate defined as the negative rate at which temperature changes with height ($^{o}C\ km^{-1}$). Some stability indices help one to visualize efficiently the potential for severe weather. Here are several ways to calculate the stability of the atmosphere:

e) Lifted Index (LI) – LI measures the instability of the atmosphere. To obtain the value, the temperature of the air parcel lifted to 500 hPa is subtracted from the temperature of the environment at 500 hPa (Table 1).
    - LI= T (environment at 500hPa) – T (parcel lifted to 500 hPa)
f) Convective Inhibition Index (CIN) – measures the total area in a Skew-T plot where the environmental temperature exceeds the parcel's temperature. It measures the negative buoyancy (meaning that external energy is required for the parcel to rises up).
g) Convective Available Potential Energy (CAPE) - For severe weather, this parameter can be very important. CAPE is the total area in a Skew-T plot where the parcel's temperature exceeds the environmental temperature. It measures the positive buoyancy accumulated over its trajectory above the LFC.
h) Equilibrium Level (EL) – EL is the level at which the temperature of the environment becomes equal to a buoyant air parcel's temperature.

❖ Charge Moment Change Network (CMCN)

Positive or negative CG strokes that are capable of producing sprites are normally associated with large charge moment changes (CMC). CMC is not measured by conventional lightning detections methods, but is perhaps the most important lightning metric for sprite researchers (Lyons et al. 2009). The CMC is defined as:

$$\Delta M_q = Z_q \times Q(t) \quad ;$$

where Z_q (km) is the altitude from which the charge is lowered to the ground and *Q(t)* (C) is the amount of charge lowered. Notice that *Q(t)* can vary in time. Sprite-parent CGs normally are large-CMC discharges (Cummer and Lyons, 2005). If the ΔM_q value is on the order of 500-1000 $C \cdot km$, then an induced dielectric breakdown in the mesosphere can occur, leading to sprites (Lyons et al. 2009). On the Relampago workstation at the National Space Science and Technology Center (NSSTC), large-CMC discharges were mapped onto radar reflectivity mosaics.

- NMQ national radar mosaics

The National Multi-Radar/Multi-Sensor System (MRMS) 3-D is a joint initiative between, NOAA's National Severe Storms Laboratory (NSSL), the Federal Aviation Administration (FAA), the National Weather Service (NWS) and the University of Oklahoma. It works using radar data which includes level 2 and level 3 data from the Weather Surveillance Radar 1988 Doppler (WSR-88D) network. The MRMS is a real-time system which integrates data from radar, gauges, lightning, satellites and profilers. It generates national products including 3-D radar reflectivity mosaics. As part of this, NOAA has developed the National Mosaic and Multi-Sensor Quantitative Precipitation Estimation (NMQ) system, available since 2009, in order to improve precipitation estimates and achieve other related goals (Zhang et al., 2011).

Developed from WSR-88D data, the result is a mosaic of reflectivity for the entire United States. For each 5-minute period, there will be data available at 31 vertical levels spaced 0.25 km near the surface stretching to 2-km spacing at the top of the grid, near 18 km.

The domain includes the conterminous U.S. as well as Puerto Rico. The grid resolution in the west-east direction is dx (lon.)= $0.01^o \approx 1.045$km at the southern bound of the domain and about 0.638 km at the northern bound of the domain. The grid resolution in north-south direction is dy (lat.) = $0.01^o \approx 1.112$km everywhere. The user can use two types of generated products: data file and images. The data file used was the 3D reflectivity mosaic grid.

- National Lightning Detection Network (NLDN)

The NLDN consists of remote and ground-based sensing stations over the United States. To detect lightning, electromagnetic methods are used. The NLDN retrieves magnetic direction finding, time-of-arrival, and electric field magnitude to provide detailed lightning data over the whole United States. NLDN devices have been modified to improve large amplitude coverage area for lightning flashes. A typical lightning detection network can provide the following information, either in real time or from archive: return stroke time (ms), estimated peak current (kA), polarity location (lat./lon.), and stroke wave form parameters. However, peak current was not considered in this study because is a poor predictor of sprites no matter what kind of lightning is involved (Lyons 2006). Flash-level NLDN data were analyzed to examine the CG characteristics of storms producing negative or positive sprite-class lightning (Lang et al. 2013).The NLDN also was used to geolocate strokes with reported impulse CMC (iCMC) values (CMC during the first 2 ms of a return stroke).

- Physical Origins of Coupling to the upper Atmosphere from Lightning (PhOCAL) forecasts

PhOCAL 2013 is a field campaign whose principal objective is to obtain high-speed videos of sprite-parent +CGs and other TLEs within a range of a three-dimensional Lightning Mapping Array (LMA). This campaign has worked in conjunction with the Upward Lightning Triggering Study (UPLIGHTS; Warner and Helsdon 2013) program and the Vaisala lightning characterization program near Concordia, KS. The operation plan is deploy/activate on forecast during any period that conditions appear promising within an LMA beginning on 20 May 2013. To get sprite times, locations and images over the Oklahoma region, operational maps and imagery were assembled into a daily file, including relevant meteorological data, iCMC and NLDN maps, summary of TLE and CG observations and status of key sensor systems. For one of the cases in this study (30 May 2012) there is no PhOCAL forecast.

- Oklahoma Lightning Mapping Arrays (OKLMA)

The LMA was developed at the New Mexico Institute of Mining and Technology (Krehbiel et al. 2000) and was modeled after the Lightning Detection and Ranging (LDAR) system developed for the Kennedy Space Center (KSC; Maier et al. 1995). OKLMA is a network of time-of-arrival sensors in central Oklahoma that receive Very High Frequency (VHF) impulses from lightning strokes. Up to thousands of points can be mapped for an individual lightning flash to reveal its location and the development of its structure.

III. Results

- 30 May 2012 case

The storm developed in western Oklahoma (Fig.3) and featured supercellular characteristics. Severe thunderstorm warnings were in place for over 5 hours. The OUN (Norman, OK) sounding was evaluated (Table 2; Fig. 4). At 04:40 UTC an active convective storm core was located in the southwestern part of the storm, where no large-iCMC (>75 C km) CGs occurred (Fig. 5a). However, the NLDN detected many negative strokes within the convective area along with a few positives between 40 to 50 dBZ, close to the convective area (Fig. 5b). As the storm moved east, the convection developed a strong core due to the environmental conditions. Around 05:00 UTC, two large positive iCMCs were reported (Figs. 5c, 6). High-speed video recorded two sprite events based upon the Hawley, TX Watec camera (Fig. 7). The sprites occurred over the precipitating anvil of the supercell associated with the cold front in northwest OK (Fig. 7-9). One minute before the first sprite, the temperature of the anvil of the storm was about -65 ºC (Figs. 3, 8), suggesting that large positive iCMCs could be related with cold temperatures in the anvil/stratiform region. At 05:15 UTC the NLDN reported 4 negative CMCs in the convective region and one in the stratiform as well as 2 positive iCMCs. At this time, one large positive CMC were reported. Also, there were 4 positives strokes dispersed over the convective region, near the convective region, and in the anvil/stratiform region.

The storm passing over OK produced a second sprite at 5:18:51 UTC. In the LMA map (Fig. 10), lightning initiated around 05:18:49.5 UTC, where convection was concentrated and developed.

One second later, two positives CGs and one negative CG in the stratiform region of the storm came to ground. Horizontal mosaics show the same positive CGs featured large iCMCs over the same area where the sprite occurred (Fig.5). Between 05:15 UTC and 05:20 UTC the storm appears to have the same basic structure.

Analyzing the sounding data, at 00:00 UTC the LCL was 819.3 hPa (Table 2), owing to low-level convergence of high-humidity air. RH at the surface was about 56% (the surface temperature was about 25.5 ºC with a dew point of 14.5 ºC), and since convergence causes rising air, RH will increase. The LFC was located at 653.1 hPa. This level is too high in the atmosphere to be supportive for tornadoes. This is because tornadoes become more likely in supercells when LFC heights are less than 2,000 m (Davis 2004). CAPE was 1592 J kg^{-1}, and the LI was -5.25. These values show an unstable environment indicating the possibility of strong thunderstorms. In the 12:00 UTC sounding (Table 2), there was a higher value for LCL, indicating a lowering of cloud base due to the moistened environment at low levels. CAPE was higher (2474 J kg^{-1}) and the CIN area was smaller. This is because the CCL value, 850 hPa, had decreased in altitude and thus the parcel of air could lift to positive buoyancy with less effort. Also, LI was more negative. The upper air map for March 30, 2012, at 12:00 UTC (Fig. 9) shows a known weather event passing thru Illinois, Missouri, Arkansas and Oklahoma approaching the south eastern United States. The wind field (10-12 m s^{-1}) coupled with the low 500-hPa dewpoint over Oklahoma implies that cloudiness dissipated after the passage of the cold front.

Two vertical cross-sections through the area of the large CMCs at 5:00 UTC were plotted (Fig. 11). In Fig. 11a, peaks of high reflectivity appear where the sprite-parent flash initiated. In the center of the core reflectivity, cloud tops were above the tropopause level. The maximum reflectivity of the storm was ranged between 50 and 75 dBZ about one minute before the first sprite occurred. In Fig. 11b, the highest reflectivity reached the stratiform region was about 40 dBZ. At 5:15 UTC (Fig. 11c) the sprite-parent +CG occurred within a light stratiform region ranging between 20 and 30 dBZ. In the convective core (Fig. 11d), strong reflectivity continued to overshoot the tropopause.

- 31 May 2013 case

During the afternoon of May 31st, multiple supercells led to the widest tornado in recorded history. The El Reno tornado touched down at 23:03 UTC, but at this time no large iCMC strokes were reported. However, hourly mosaics showed many large positive iCMCs (> 75 C km) occurred within the storm during the hour following tornado touchdown (Fig.12a). However, the dominant polarity for total CGs I the storm appeared to remain negative (Fig. 12b). According to the PhOCAL forecast discussion, significant convection had advected moisture over OK, leading to the developing of significant supercells, then MCSs in mid OK.

Analyzing the sounding data (Fig. 13, Table 3), at 12:00 UTC the LCL was 924 hPa and the CAPE was 2,856 J kg^{-1}. In other words, there was an LCL close to the surface and there was a large CAPE area, both of which increase the probability of tornado formation. Also, high humidity near the surface, 72.7%, combined with heat (75 ºF) improved chances of tornado-genesis. An LI of about -4.0 shows a very unstable atmosphere, with the likelihood for severe thunderstorms. However, LFC was 677.2 hPa with a CIN of -243 J kg^{-1} and these values were not

as supportive of tornado formation. The June 1st sounding data at 00:00 UTC (Table 3) showed weather conditions were slightly different. The LCL was at a higher altitude, 876.9 hPa, where there were no convective clouds in the area. However, the CAPE was 3018 J kg^{-1} and the LI was -6.5, indicating a very unstable atmosphere. In summary, these soundings data suggests that the environment was favorable for severe thunderstorm development along with possible tornadoes.

A minute before the tornado, over 65 dBZ radar reflectivity was observed (Fig. 14a). Comparing with the IR image Fig 14b, there was a line of cold clouds over OK, KS and MO. The hourly radar/lightning plot (Fig. 12a) shows large positive iCMC discharges in the area of coldest cloud tops, where the temperature was ranging between -50 ºC and -64 ºC for the area where the tornado occurred. Looking at the surface map (Fig. 15), there was an upper-level trough associated with a cold front, where unstable air mass was expected. The sky cover was broken. The temperature was 82 ºF and the dewpoint was 79 ºF. However, the upper air map (Fig. 16) shows significant upper-level flow, with a wind magnitude of 28.30 ms^{-1} and a dewpoint of -23 ºC at 500 hPa. Vertical radar cross section (Fig. 12c) shows wide area of reflectivity exceeding the tropopause level due to the strong updraft, 2 minutes before the tornado touched down.

- 1 June 2013 case

According to the PhOCAL forecast, supercells gradually evolved into linear MCS over NE OK (Fig. 17a). The radar shows an east-west oriented bowed convective line containing high-reflectivity cells. An hourly mosaic of reflectivity was produced at 07:00 UTC, where the convective mass was located in the east of Oklahoma with many large negatives iCMCs reported (Fig. 18a). These large negative iCMC discharges (>75 C km; -iCMCs) mainly occurred in the convective line. Large positive iCMC discharges (+iCMCs) were scattered in the stratiform regions of the storm. The leading convective line moved southeastward with the stratiform rain trailing behind. The NLDN (Fig. 18b) shows most of the negatives concentrated in the convective line where large negatives iCMCs occurred (Fig. 18c). Positives CGs also were scattered in the convective line and negatives were scattered in the convective line, but the large-iCMC positives occurred mainly in the stratiform region (Fig. 18c). Storm shape was essentially symmetric, a classic leading line/trailing stratiform MCS. A cross section was plotted in one area where large negative iCMCs occurred (Fig. 18d). Reflectivity was exceeded 50 dBZ in many of these convective cells in the southern part of the storm. The eastern part of OK featured strong convective development where cloud top temperatures reached -64 ºC (Fig. 17b). There was 6 negatives iCMCs were reported (Fig. 18c) a few minutes before the IR image time. The surface map (Fig. 19) showed that the OK convection was associated with the low level trough coming from the Gulf of Mexico and bringing in moisture. This trough was associated with a stationary front. Skies were completely overcast over the OK eastern region with a surface wind magnitude of 0.51 m s^{-1}.

Around this time, large iCMCs were divided into separate groups in and near the convective line (Figs. 18, 20). The stratiform region was accompanied by numerous convective cells. Maddox (1980) noted that the largest and most intense mesoscale convective complexes were characterized by stratiform rain in their mature and dissipating stages. Large positive iCMCs were scattered in this area, while –iCMCs prevailed in the convection region located in the southern

component of the storm (Figs. 18, 20). There was a frequent large iCMC activity around this time (Fig. 20). Afterward, the reflectivity generally fell as the mesoscale system weakened and dissipated while moving through eastern OK.

IV. Conclusions

The radar, satellite, sounding data and lightning behavior of three storms that produced significant large-iCMC (> 75C km) lightning strokes that often can produce sprites to sprite have been analyzed. Tables 2 and Table 3 show an overview of the atmospheric stability of the three storms. During the early morning of March 30, 2012, two sprite events occurred in the precipitating stratiform anvil of a supercellular thunderstorm. All cases had high CAPE and negatives LI values. The minimum cloud-top temperatures in the observed cases ranged from -64 ºC and up. The IR image for 30 March case showed that the sprites occurred in cold cloud-top areas of the storm, and the parent lightning initiated in the convective core where the maximum radar reflectivity was present. The March 30th, storm produced more large-positives iCMCs than negatives. Furthermore, large positive iCMC strokes in the stratiform of the storm produced sprites. The LMA data for 05:18 UTC sprite-parent lightning on March 30th view of regions of charge that were involved in the lightning flashes. The flash first originated in the convection and then propagated out into the stratiform region before producing the sprite-parent +CG. LMA quality for this case was reduced due to large distance between the sensors and the weather event.

The 31 May 2013 storm also formed in a moist, unstable environment. The El Reno tornado formed under the coldest cloud-top area of the convective core. An hourly mosaic analysis of the May 31st tornadic-storm showed that it produced more large positive than negative iCMCs, and these mainly occurred in convection. By contrast, after the storm had grown into an MCS on June 1st it produced primarily negative large-iCMC strokes in the convective line and primarily positives in the stratiform region. During the 31 May case, after the tornado development the storm produced many large iCMC discharges in the convective core. All large-iCMC storm featured intense vertical reflectivity development with cloud tops breaking through the tropopause level. These storms appeared to have normal polarity charges structures, with negatives CGs concentrated in the convective core and positive CGs in the light stratiform areas of the storm.

VI. Acknowledgements

This work was supported by the USRA corporation and MSFC/NASA though the TRMM-LIS program. The first author thanks Timothy Lang, my mentor, for help with the data acquisition and analysis and for supplying this wonderful opportunity, and thanks to Rita and David for help with the Relampago computer workstation. I also want thank the SPoRT team for the use of their facilities, and my lab partners: Ethan, Brett, Tony, Rachel and Jordan.

VII. References

Carey, Lawrence D., et al. "Lightning location relative to storm structure in a leading-line, trailing-stratiform mesoscale convective system." *Journal of Geophysical Research: Atmospheres (1984–2012)* 110.D3 (2005).

Cummer, Steven A., et al. "ELF radiation produced by electrical currents in sprites." *Geophysical Research Letters* 25.8 (1998): 1281-1284.

Cummer, Steven A., and Walter A. Lyons. "Implications of lightning charge moment changes for sprite initiation." *Journal of Geophysical Research: Space Physics (1978–2012)* 110.A4 (2005).

Davies, Jonathan M. "Estimations of CIN and LFC associated with tornadic and nontornadic supercells." *Weather and forecasting* 19.4 (2004): 714-726.

Fritsch, J. M., R. J. Kane, and C. R. Chelius, 1986: The contribution of mesoscale convective weather systems to the warm-season precipitation in the United States. *J. Climate Appl. Meteor.,* **25**(10), 1333-1345.

Fujita, T. T.,1992: The mystery of severe storms. WRL Research Paper 239, Dept. of Geophysical Sciences, University of Chicago, 298 pp. [NTIS PB-182021.]

Goodman, Steven J., and Donald R. MacGorman. "Cloud-to-ground lightning activity in mesoscale convective complexes." *Monthly weather review* 114.12 (1986): 2320-2328.

Houze, R. A., B. F. Smull, and P. Dodge, 1990: Mesoscale organization of springtime rainstorms in Oklahoma. ***Mon. Wea. Rev.***, **118**, 613–654.

Jayaratne, E. R., and C. P. R. Saunders. "Thunderstorm electrification: The effect of cloud droplets." *Journal of Geophysical Research: Atmospheres (1984–2012)* 90.D7 (1985): 13063-13066.

Lang, Timothy J., et al. "The severe thunderstorm electrification and precipitation study." *Bulletin of the American Meteorological Society* 85.8 (2004): 1107-1125.

Lang, T.J., S.A.Cummer, S.A. Rutledge, and W.A.Lyons, 2013: The meteorology of negative cloud-to-ground lightning strokes with large charge moment changes: Implications for negative sprites. *J. Geophys. Res. Atmos.*, 118, doi:10.1002/jgrd.50595.

Lyons, W. A., 2006: The meteorology of transient luminous events – An introduction and overview. *NATO Advanced Study Institute on Sprites, Elves and Intense Lightning Discharges*, M. Fullekrug et al. (eds.), Springer, 19-56.

Lyons, W. A., M. Stanley, J. D. Meyer, T. E. Nelson, S. A. Rutledge, T. J. Lang, and S. A. Cummer, 2009: The meteorological and electrical structure of TLE-producing convective storms. In *Lightning: Principles, Instruments and Applications*, H.D. Betz et al. (eds.), 389-417 pp., Springer Science+Business Media B.V., DOI: 10.1007/978-1-4020-9079-0_17.

Lyons, Walter A. "Sprite observations above the US High Plains in relation to their parent thunderstorm systems." *Journal of Geophysical Research* 101.D23 (1996): 29641-29.

Lyons, Walter A., et al. "Characteristics of sprite-producing positive cloud-to-ground lightning during the 19 July 2000 STEPS mesoscale convective systems." *Monthly weather review* 131.10 (2003): 2417-2427.

Maier, L., C. Lennon, T. Britt, Lightning detection and ranging (LDAR) system performance analysis. Proceedings of 6th Conference on Aviation Weather Systems, Am. Meteorol. Soc., Boston, Mass., 1995.

Meyer, Tiffany C., et al. "Radar and lightning analyses of gigantic jet-producing storms." *Journal of Geophysical Research: Atmospheres* (2013): 1-19.

Ray, P. S., 1986: *Mesoscale meteorology and forecasting*. Amer. Meteor. Soc., Boston, MA, 793 pages.

Saunders, C. P. R., W. D. Keith, and R. P. Mitzeva. "The effect of liquid water on thunderstorm charging." *Journal of Geophysical Research: Atmospheres (1984–2012)* 96.D6 (1991): 11007-11017.

Saunders, C. P. R., and I. M. Brooks (1992), The effects of high liquid water content on thunderstorm charging, J. Geophys. Res., 97(D13), 14671–14676, doi:10.1029/92JD01186.

Takahashi, Tsutomu. "Electrical properties of oceanic tropical clouds at Ponape, Micronesia." *Monthly Weather Review* 106.11 (1978): 1598-1612.

Thomas, Ronald J., et al. "Comparison of ground-based 3-dimensional lightning mapping observations with satellite-based LIS observations in Oklahoma."*Geophysical research letters* 27.12 (2000): 1703-1706.

Warner, Tom A., et al. "UPLIGHTS: Upward Lightning Triggering Study."*Bulletin of the American Meteorological Society* (2012).

Zhang, J., and Coauthors, 2011: National Mosaic and Multi-Sensor QPE (NMQ) System: Description, results, and future plans. *Bull. Amer. Meteor. Soc.*, **92**, 1321–1338.

V. Tables

Table 1. Common ranges of LI and CAPE (J kg^{-1}) for various atmospheric stability scenarios.

Stability	LI	CAPE
Stable	0 to ≥+3	< 0
Moderated Unstable	-4 to 0	0 to 2500
Unstable	-6≤ to -4	2500 to ≥3500

Table 2. Sounding parameters for 30 March 2012 storm.

MARCH 30TH 2012								
Time (UTC)	**RH(%)**	**LCL(hPa)**	**CCL(hPa)**	**LFC(hPa)**	**LI(ºC)**	**CIN(J/kg)**	**CAPE(J/kg)**	**EQ(hPa)**
00:00:00	56	819.3	740	653.1	-5.25	-166	1592	224.8
12:00:00	80	936.8	850	740	-6.5	-28.4	2474	218.9

Source:University of Wyoming. Sounding: Norman,Oklahoma.

Table 3. Sounding parameters for 31 May 2013 storm.

MAY 31st 2013								
Time (UTC)	**RH(%)**	**LCL(hPa)**	**CCL(hPa)**	**LFC(hPa)**	**LI(ºC)**	**CIN(J/kg)**	**CAPE(J/kg)**	**EQ(hPa)**
12:00:00	93	924	755	677.2	-4.0	-243	2856	180.9
00:00:00 *	73	876.9	760	711.8	-6.5	-120	3018	M**

*Source:University of Wyoming. Sounding: Norman,Oklahoma. *June 1st sounding data **Missing data*

VI. Figures

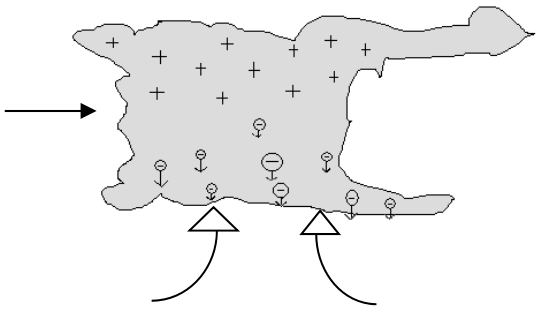

Figure 1. This illustrative picture represents a general overview of non-inductive charging. Where large precipitation-sized rimed ice collides with ice crystals, it commonly acquires net negative charge and the smaller ice crystal gain net positive charges. Thus, by gravity and also by convection, larger hydrometeors come down toward thunderstorm base while smaller hydrometeors are lofted toward thunderstorm top by updrafts.

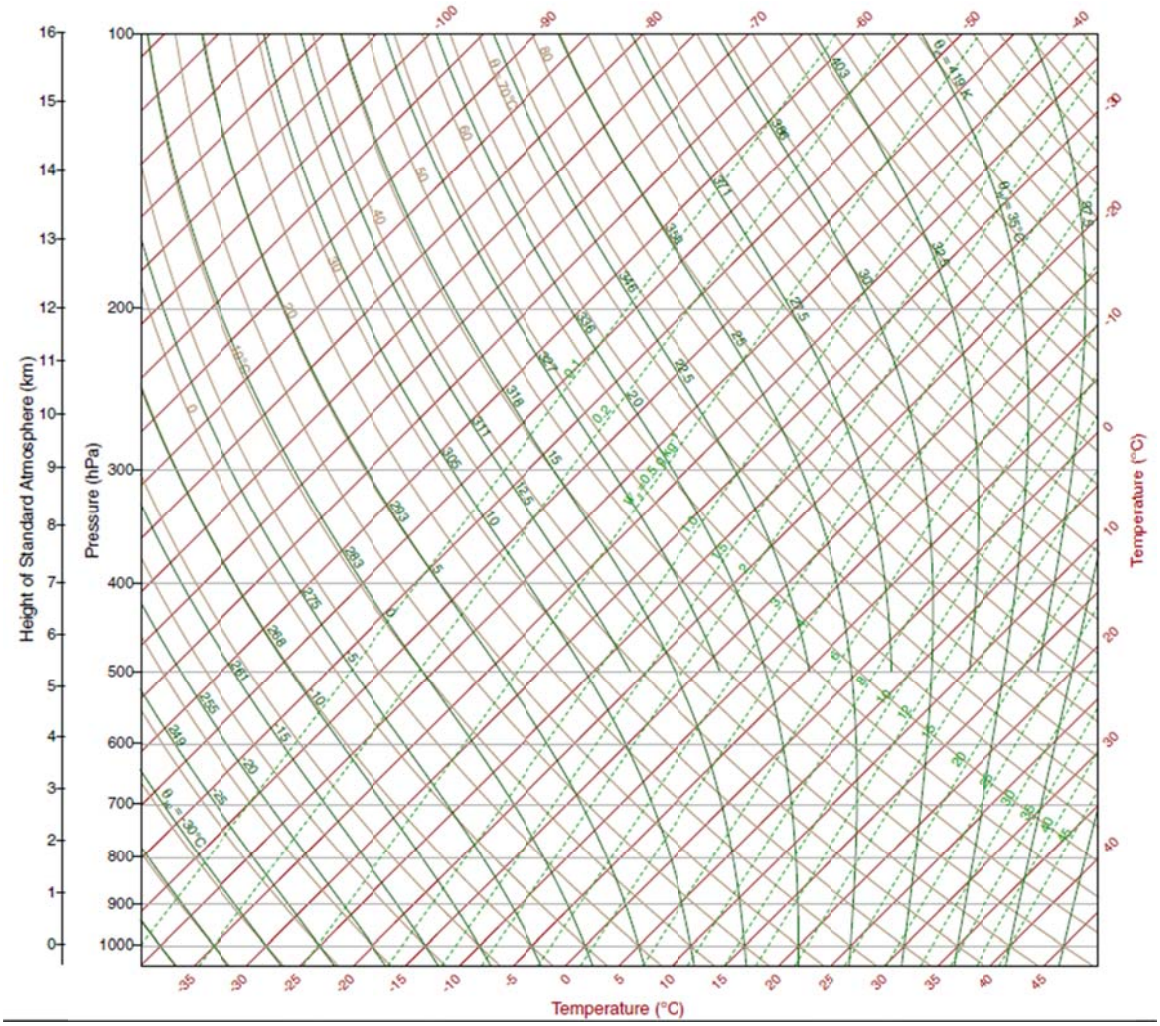

Figure 2. A blank Skew-T chart. To describe the Skew-T we need to understand the meaning of its lines. Isobars are horizontal straight lines that indicate constant pressure. Isotherms indicate the temperature in straight lines that runs diagonally upward from left to right. The mixing ratio is a measure of mass of water vapor relative to the mass of other gases in the atmosphere. In the Skew T, constant saturated mixing ratio is represented by green dashed lines.

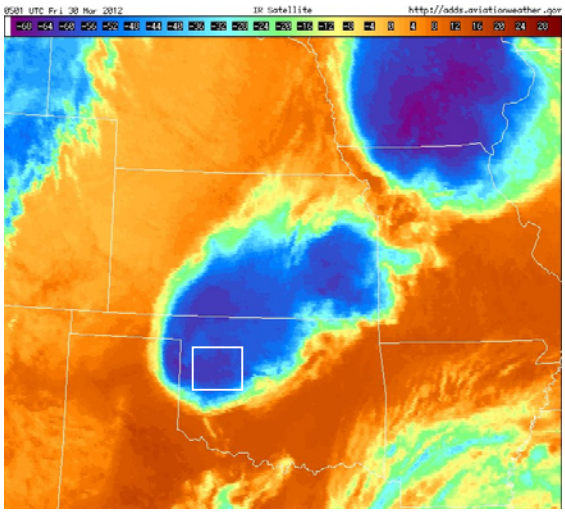

Figure 3. IR image for 30 March 2012 at 05:01 UTC (a minute before the sprite). The most likely location of the sprite is within the white box, over some of the coldest cloud tops in the storm.

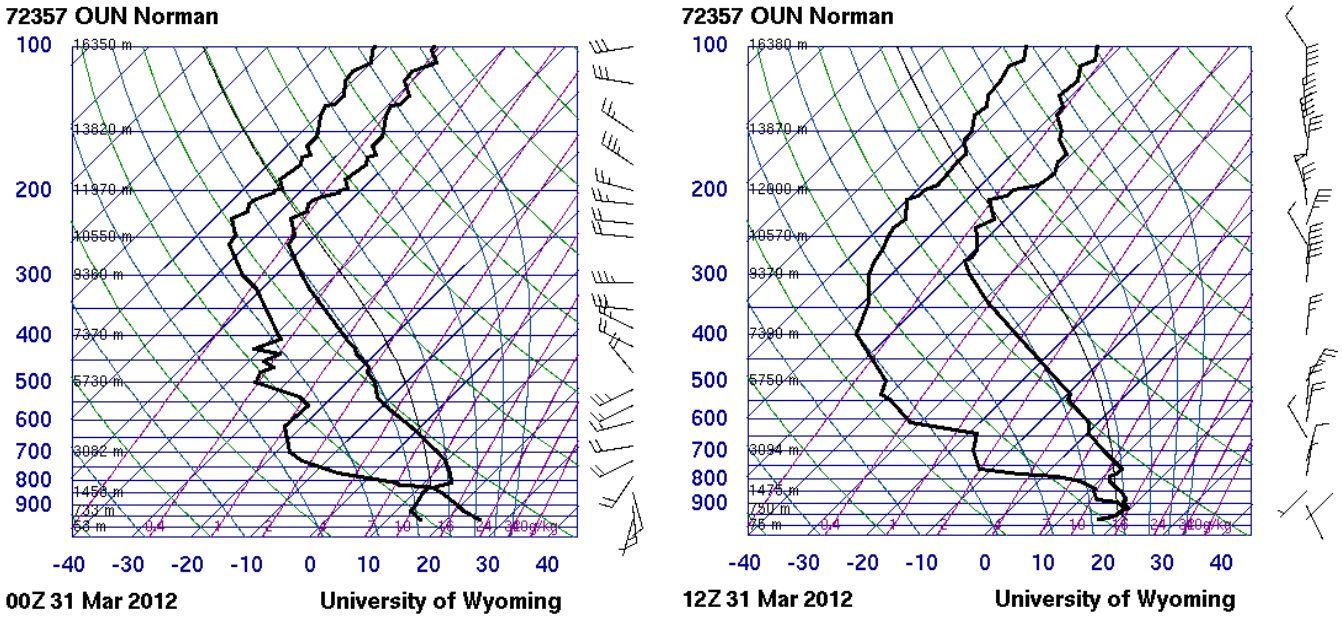

Figure 4. Skew-T diagram from Norman, Oklahoma, at 00:00 UTC (left) and 12:00 UTC (right) of 31 March 2012.

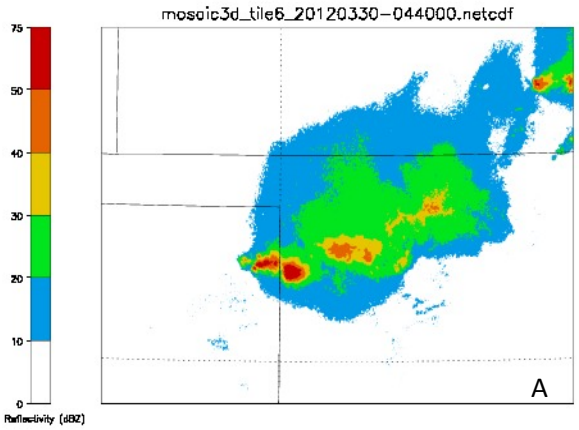
mosaic3d_tile6_20120330-044000.netcdf
75
50
40
30
20
10
0
Reflectivity (dBZ)
A

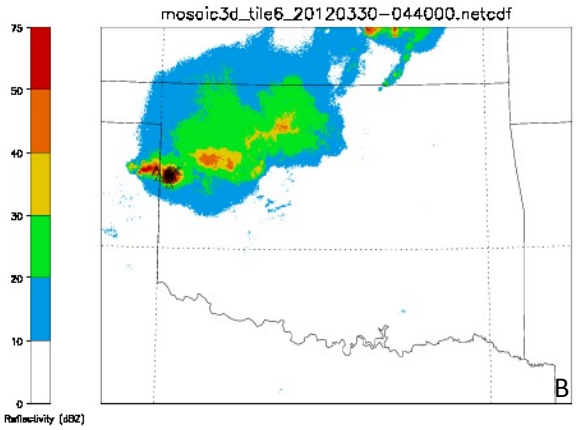
mosaic3d_tile6_20120330-044000.netcdf
75
50
40
30
20
10
0
Reflectivity (dBZ)
B

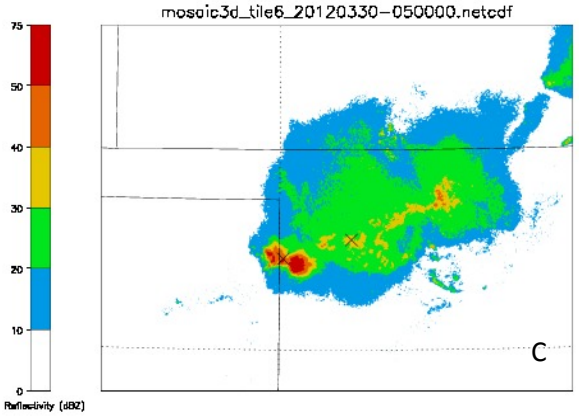
mosaic3d_tile6_20120330-050000.netcdf
75
50
40
30
20
10
0
Reflectivity (dBZ)
C

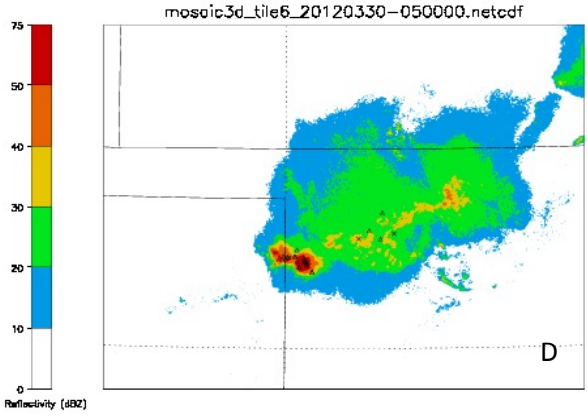
mosaic3d_tile6_20120330-050000.netcdf
75
50
40
30
20
10
0
Reflectivity (dBZ)
D

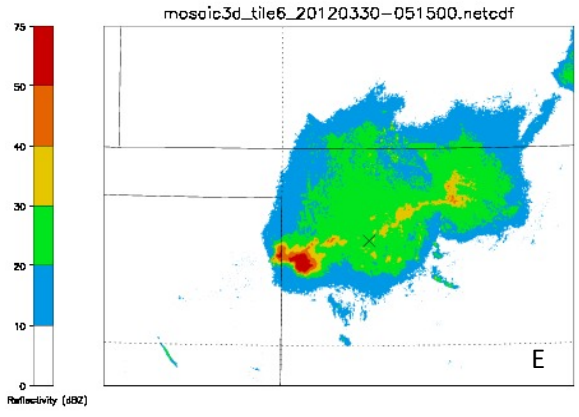
mosaic3d_tile6_20120330-051500.netcdf
75
50
40
30
20
10
0
Reflectivity (dBZ)
E

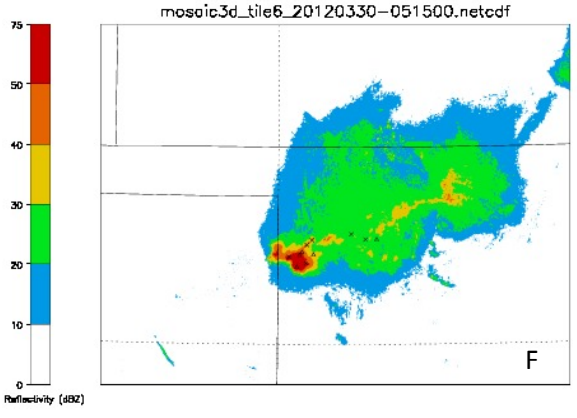
mosaic3d_tile6_20120330-051500.netcdf
75
50
40
30
20
10
0
Reflectivity (dBZ)
F

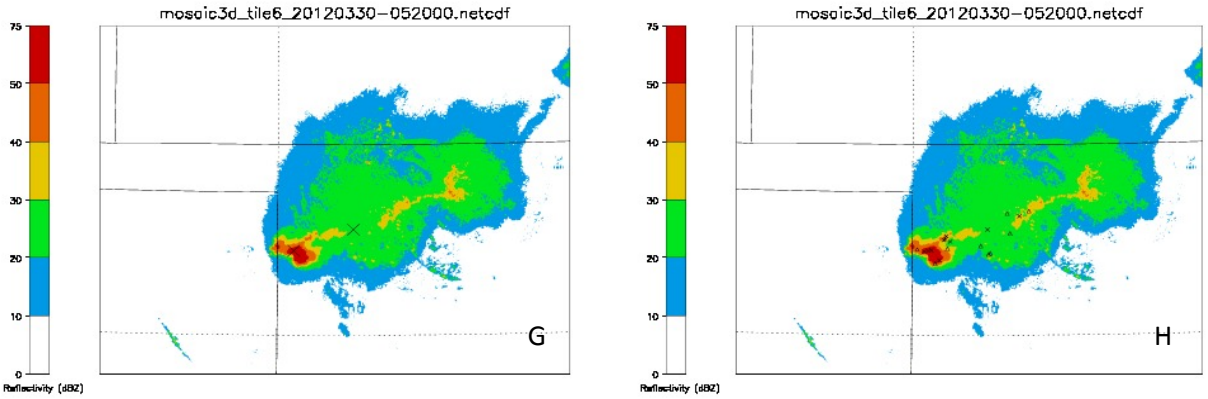

Figure 5. Radar and lightning evolution of the 30 March 2012 storm over western Oklahoma. (A), (C), (E), and (G) show composite radar reflectivity and large iCMC (>75 C km) discharges (positives are X symbols, negatives are triangles). (B), (D), (F) and (H) show composite radar reflectivity along with NLDN-detected CGs (positives are X symbols, negatives are triangle). Five minutes of radar and lightning data for 04:40 UTC are shown in (A) and (B). (C) and (D) are the same as (A) and (B) but for 05:00 UTC. (E) and (F) are for 05:15 UTC, and (G) and (H) are for 05:20 UTC.

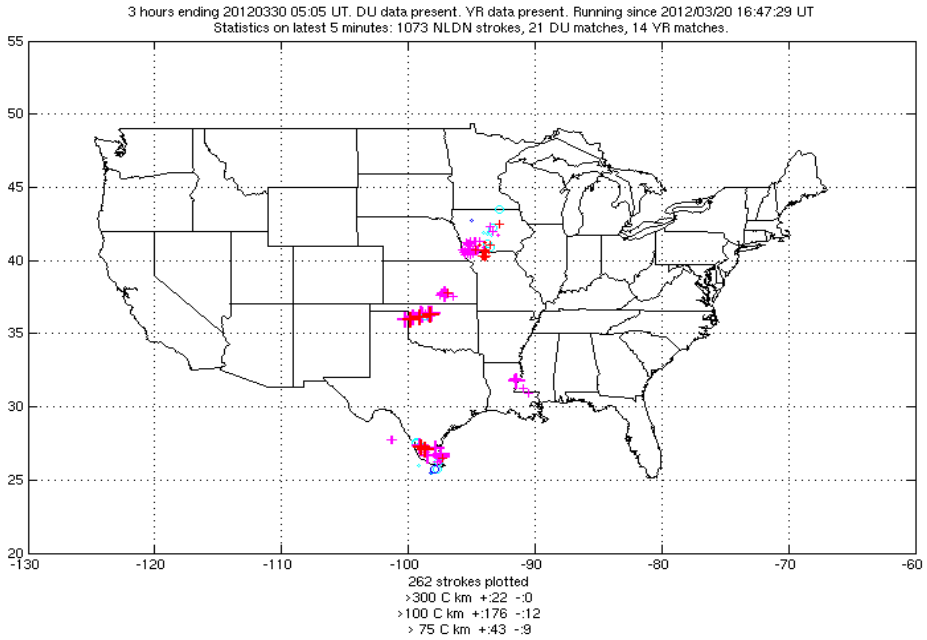

Figure 6. All large-iCMC discharges for the three-hour period before 05:05 UTC in different locations. Positives are red plus signs, negatives are blue circles. Note the big +CMCs discharges in western OK associated with the storm studied here.

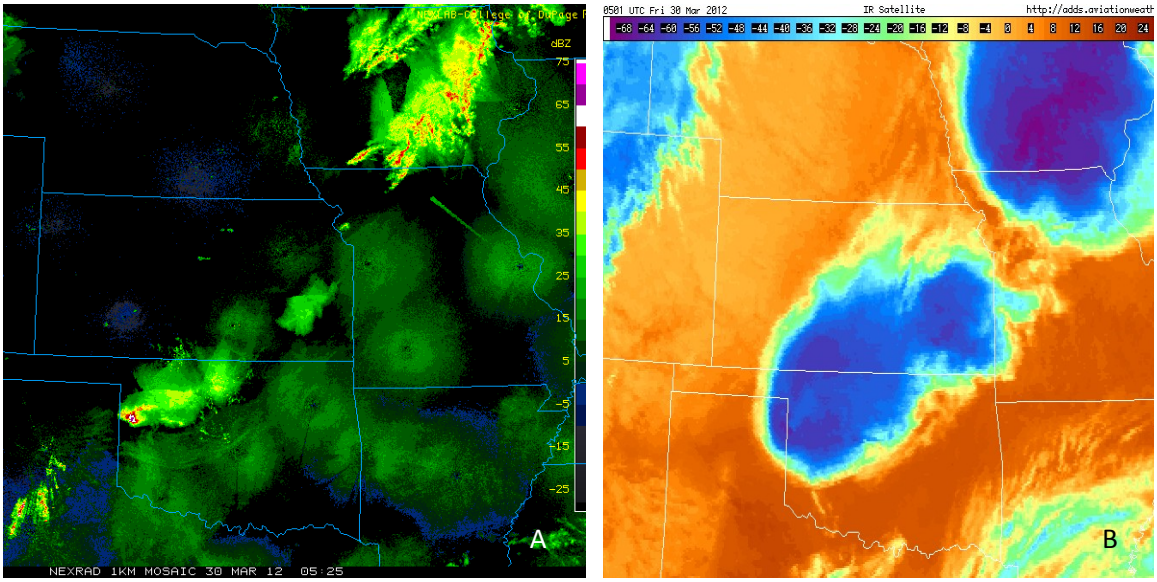

Figure 7. Radar (A) and Infrared (IR) composites (B) of the Oklahoma storm. (A) Radar image shows a strong convective core in western OK at 05:25 UTC. (B) Infrared image of Oklahoma storm at 05:01UTC on 30 March 2012. The convective cloud tops over OK had temperatures ranging between -50 ºC and -64 ºC.

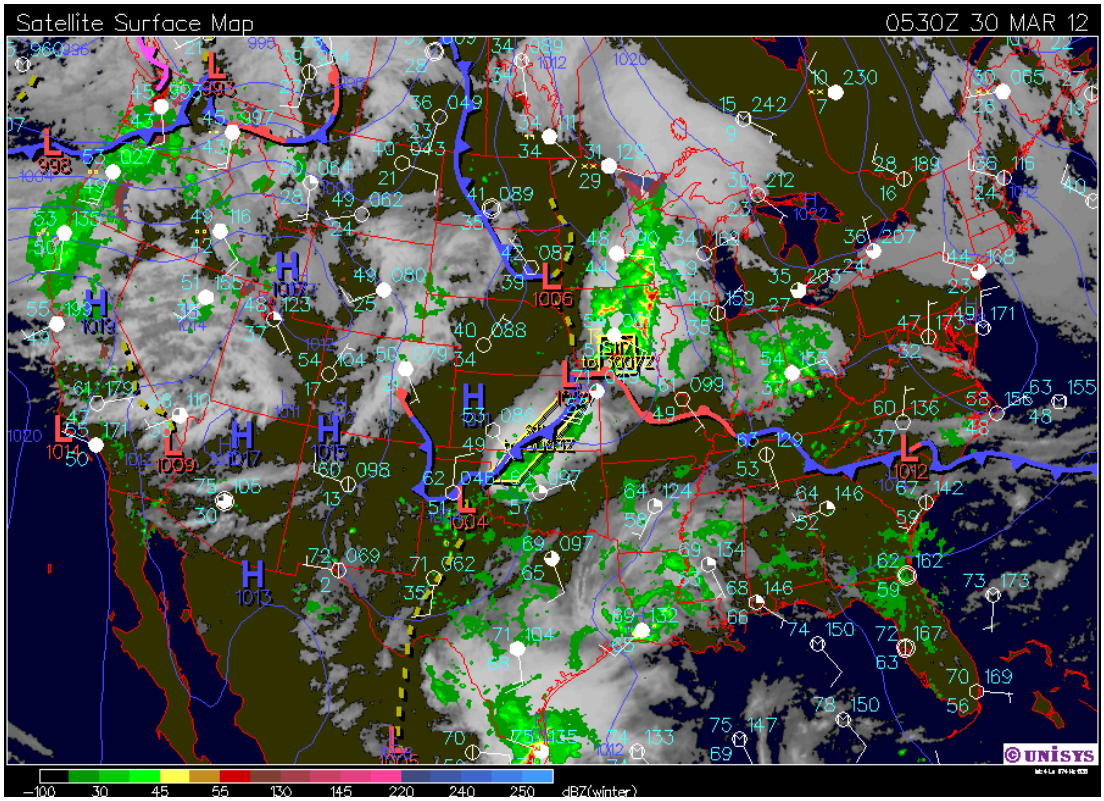

Figure 8. Surface map showing western OK affected by the cold front. At 05:30 UTC a severe thunderstorm warning was issued for this region.

30 March 2012: Upper Air 500hPa

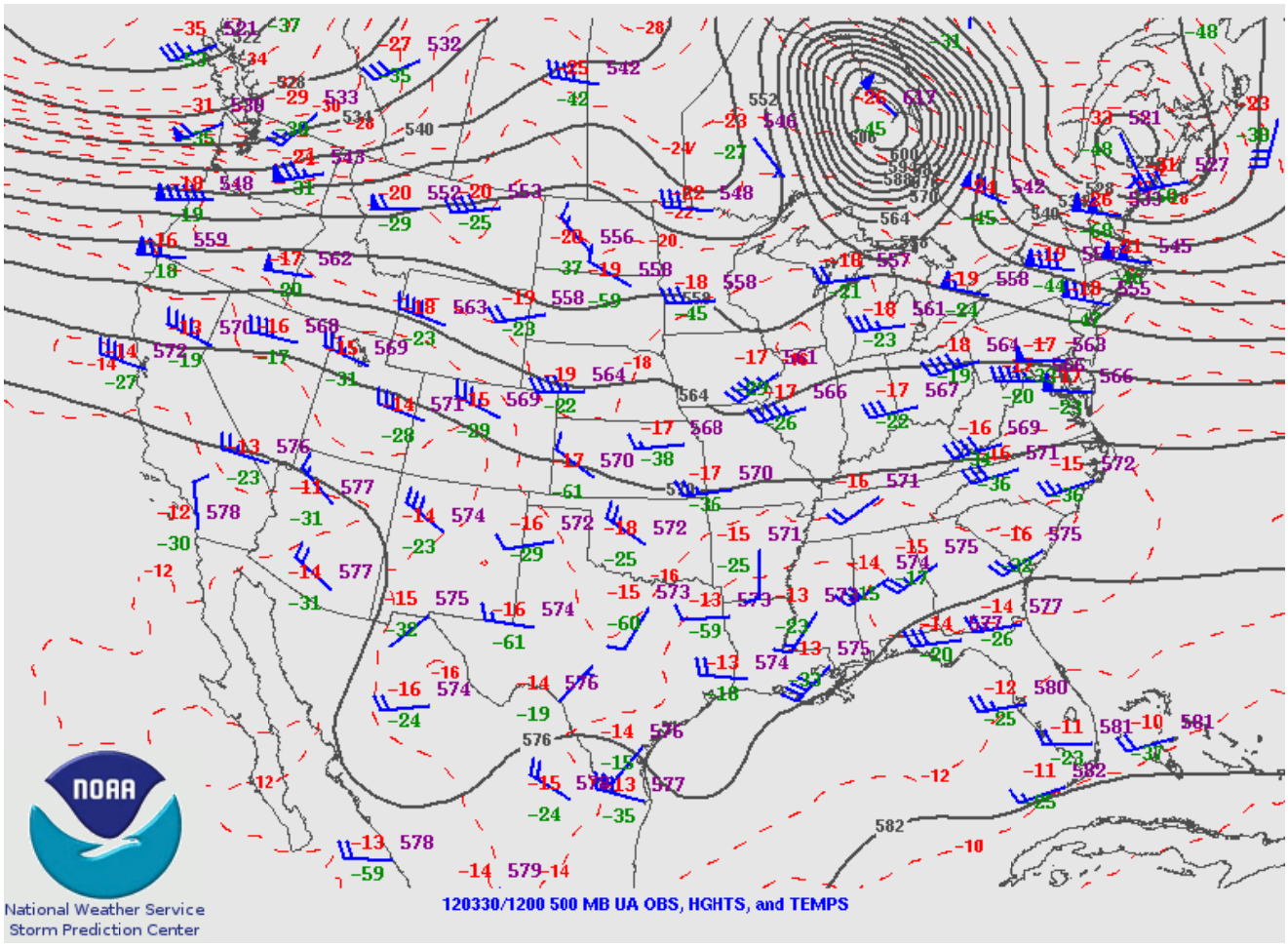

Figure 9. Upper air station model for OK shows a temperature near -18 ºC. The dewpoint was around -25 ºC with wind speeds ranging between 13 m s^{-1} from the NW.

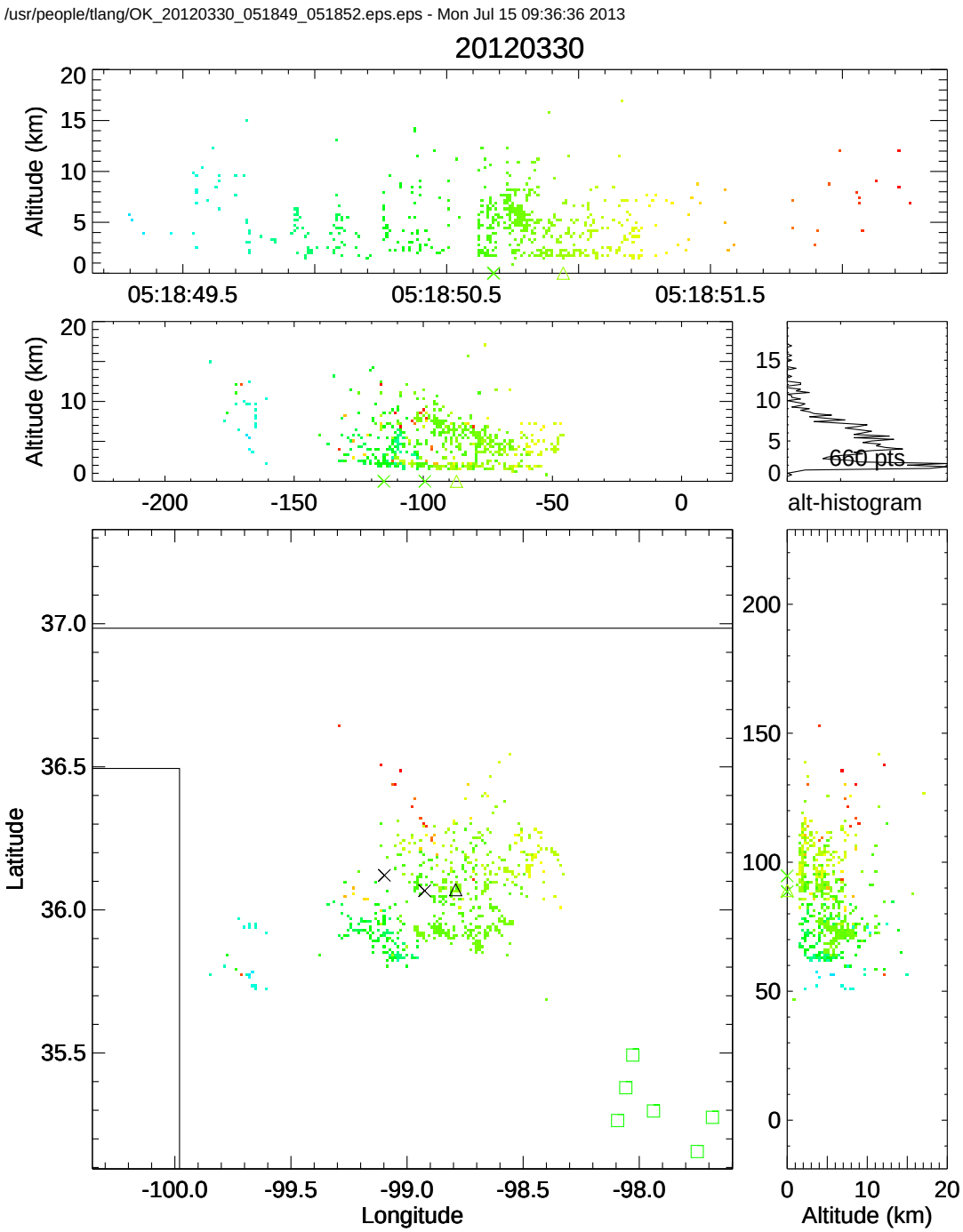

Figure 10. 30 March 2012 observed sprite-parent lightning flash that originated at about 05:18:49 UTC. (1) Altitude (km) versus Time (s), (2) Altitude (km) versus longitude (km), (3) Normalized altitude (km) histogram of Very High Frequency (VHF) sources, (4) Latitude (km) versus Longitude (km), and (5) latitude (km) versus altitude (km). Color coding indicates elapsed time, with blue representing the earliest time and red the latest time.

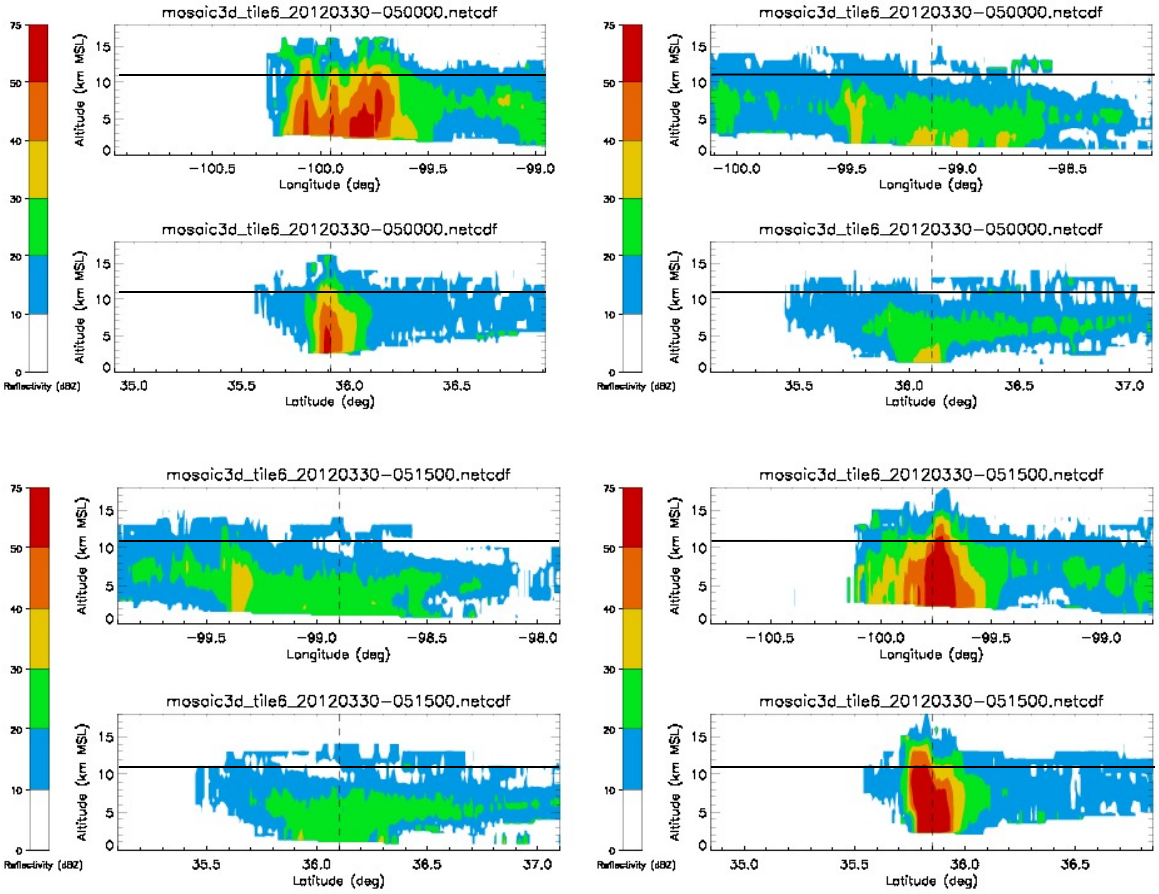

Figure 11. (A) and (B) vertical cross sections for 30 March 2012 through the locations of the two large CMCs at 05:00 UTC. (A) iCMC in the core reflectivity. (B) iCMC in the stratiform region of the storm. (C) and (D) are vertical cross sections at 05:15 UTC: (C) iCMC in the stratiform region and (D) Vertical cross section in the core reflectivity. Horizontal black lines represent the tropopause at 224.8 mb.

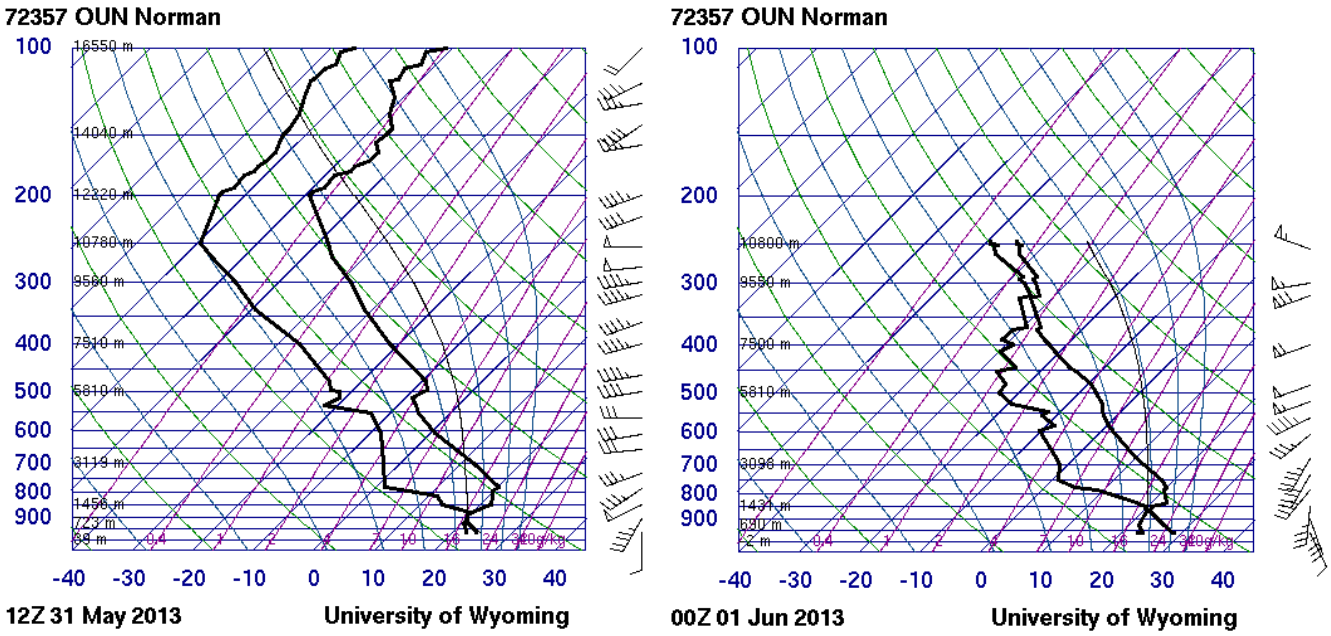

Figure 12. Skew-T diagram from Norman, Oklahoma, at 00:00 UTC (left) of 31 May 2013 and 12:00 UTC (right) of 1 June 2013.

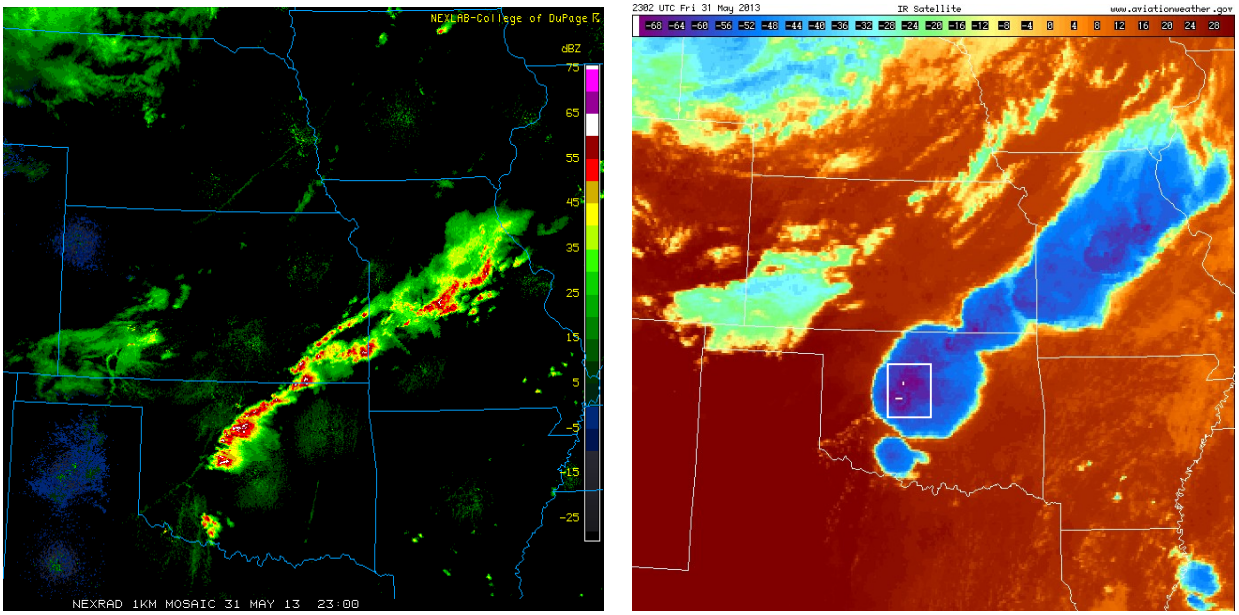

Figure 13. Radar (A) and Infrared (B) composites of the 31 May 2013 Oklahoma storm. (A) Radar image shows a strong convective line in the mid OK at 23:00 UTC. (B) Infrared image of Oklahoma storm at 23:02 UTC on 31 May 2013. The convective cloud tops over OK had temperatures ranging between -50 ºC and -64 ºC. In the center of the white box, temperature reach bellow -68 ºC. Over this region the El Reno tornado was about to touch down.

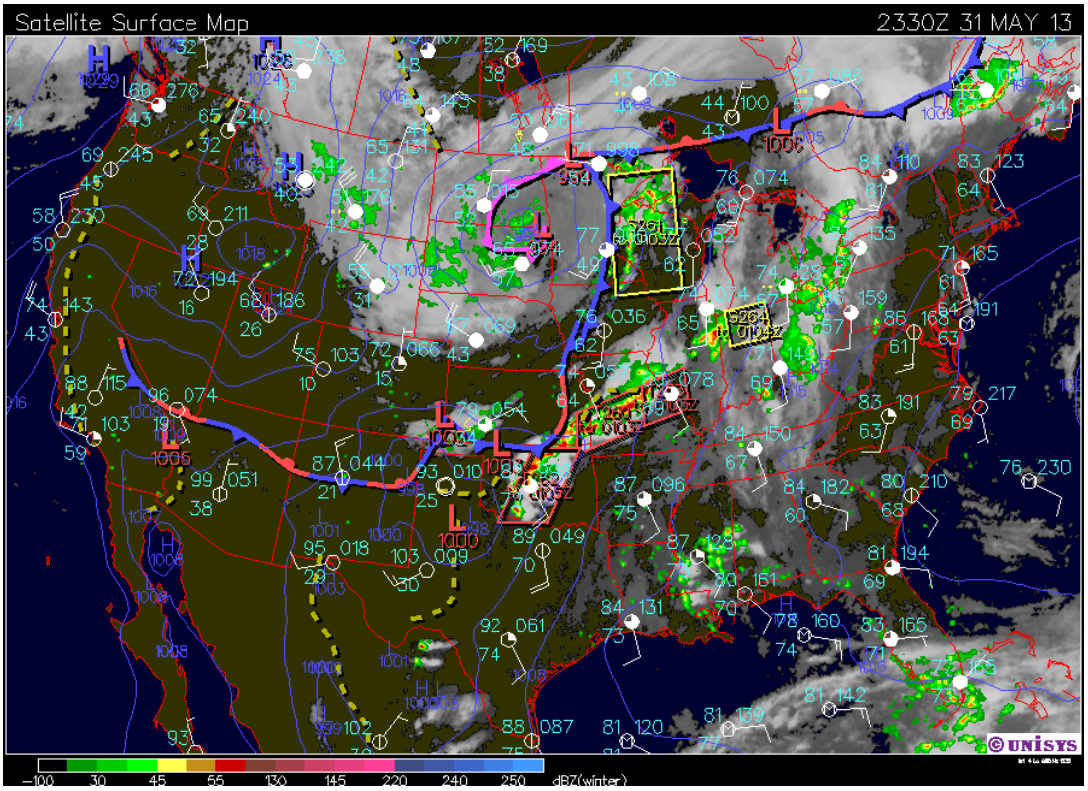

Figure 14. Surface map showing the mid-south OK affected by a cold front. At 23:30 UTC a tornado warning was issued across the entire convective line due to the front.

1 June 2013: Upper Air 500hPa

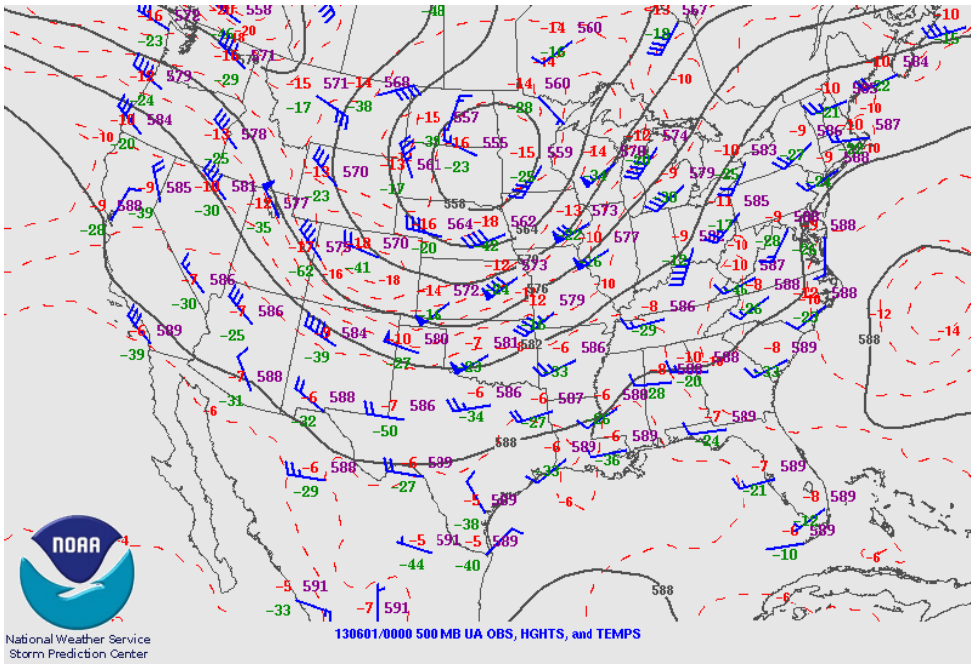

Figure 15. Upper air station map for OK shows unstable weather where the temperature was -18 ºC, the dewpoint was around -25 ºC with wind speeds ranging between 20.58 m s^{-1} from W to SW.

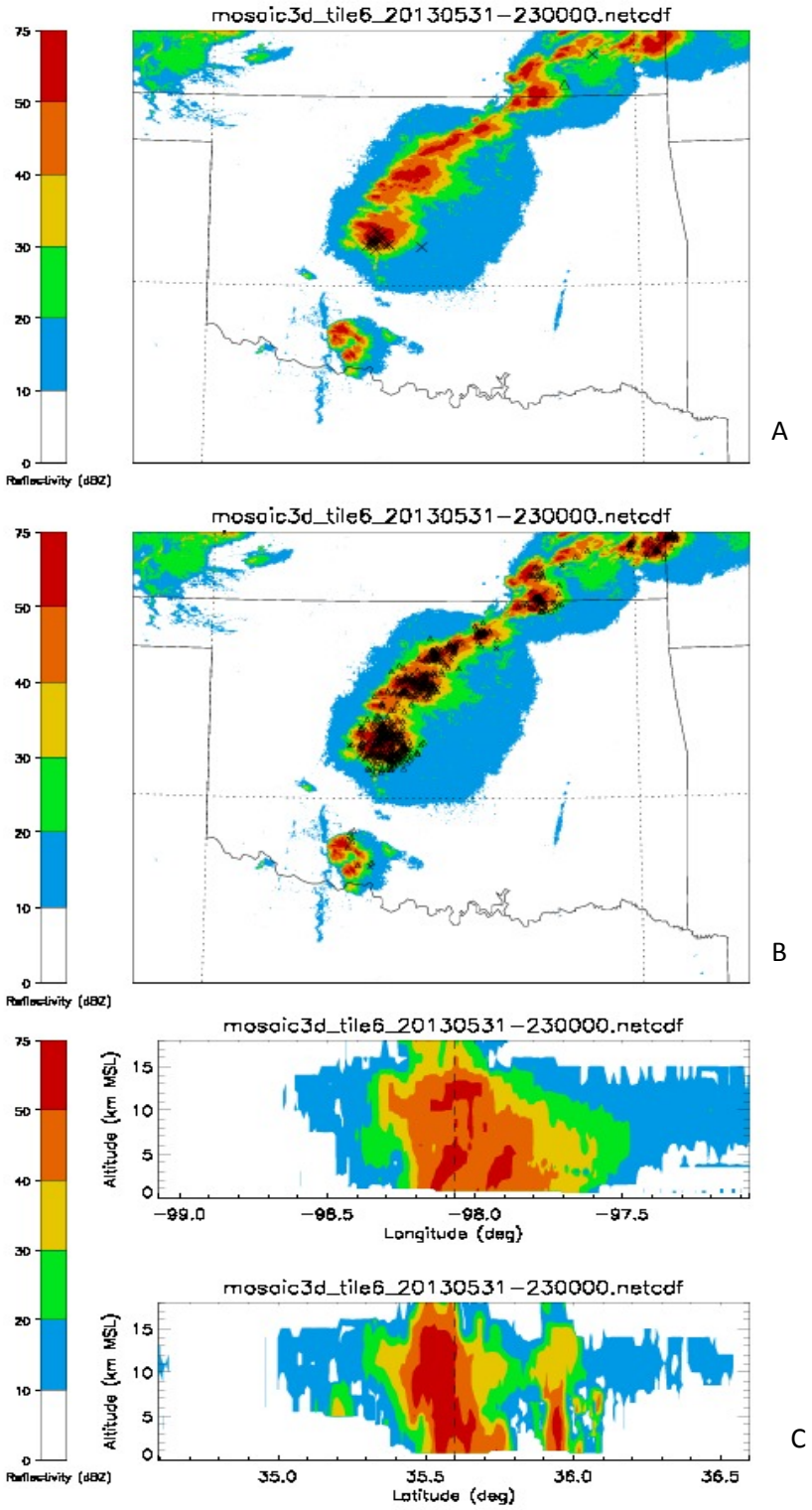

Figure 16. A) 31 May 2013 shows an hourly composite radar reflectivity and large CMC (>75 C km) discharges over OK (positive are X symbols and negative are triangle symbols). (B) shows represent vertical cross section of the deep convection for the El Reno Tornado event. The black line represents the tropopause at 180.9mb.

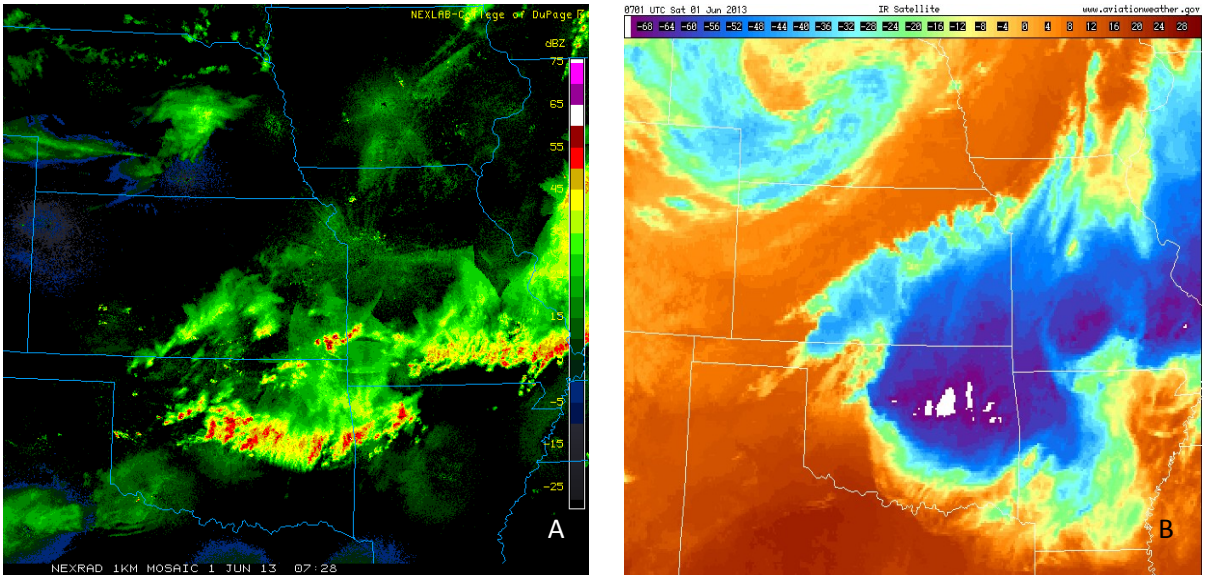

Figure 17. Radar (A) and Infrared (B) composites of the 1 June 2013 Oklahoma storm. (A) Radar image shows the convective line in the eastern OK at 07:28 UTC. (B) Infrared image of Oklahoma storm at 7:01 UTC on 1 June 2013. The convective cloud tops over OK had temperatures over -64 ºC.

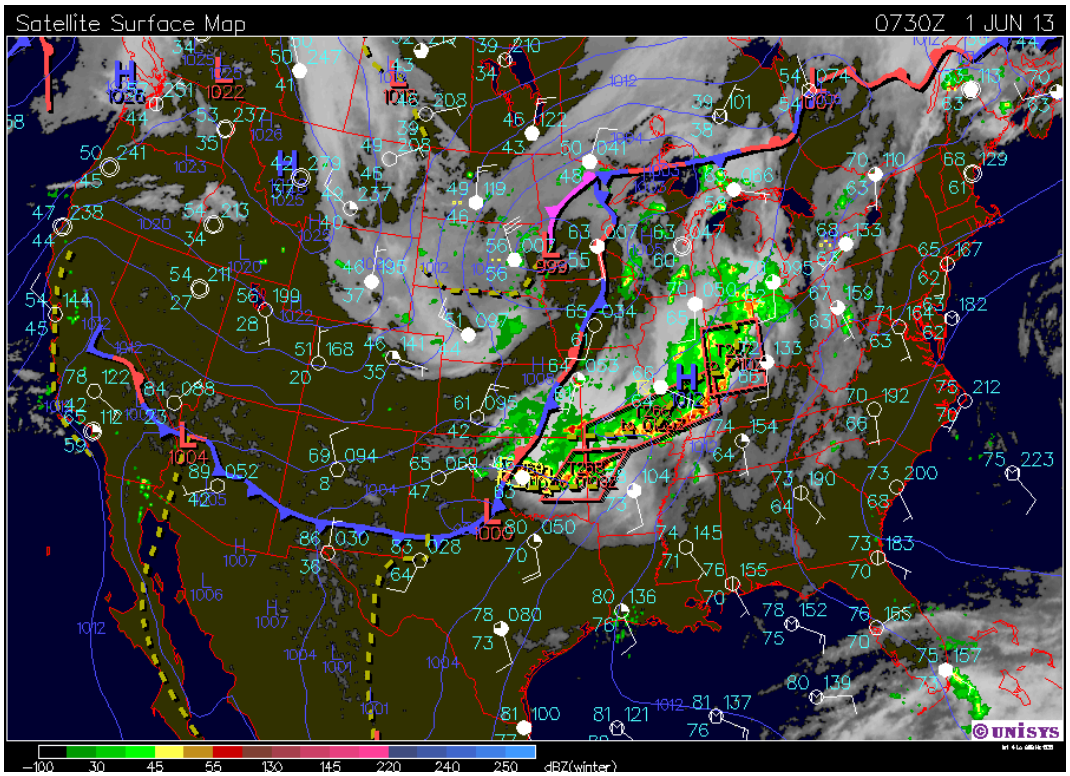

Figure 18. Surface map showing the mid-south OK affected by a stationary front. At 07:30 UTC a tornado and severe thunderstorm warning was issued across the entire convective line due to the front.

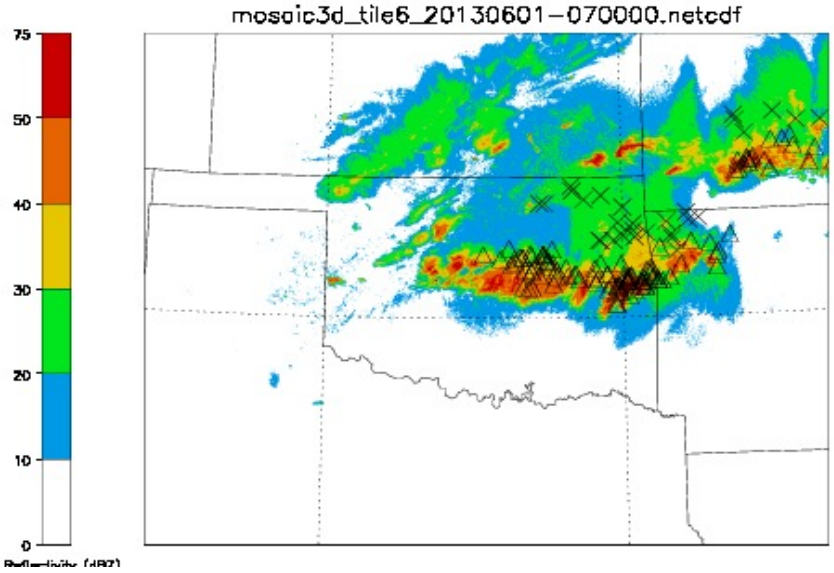
mosaic3d_tile6_20130601-070000.netcdf
75
50
40
30
20
10
0

A

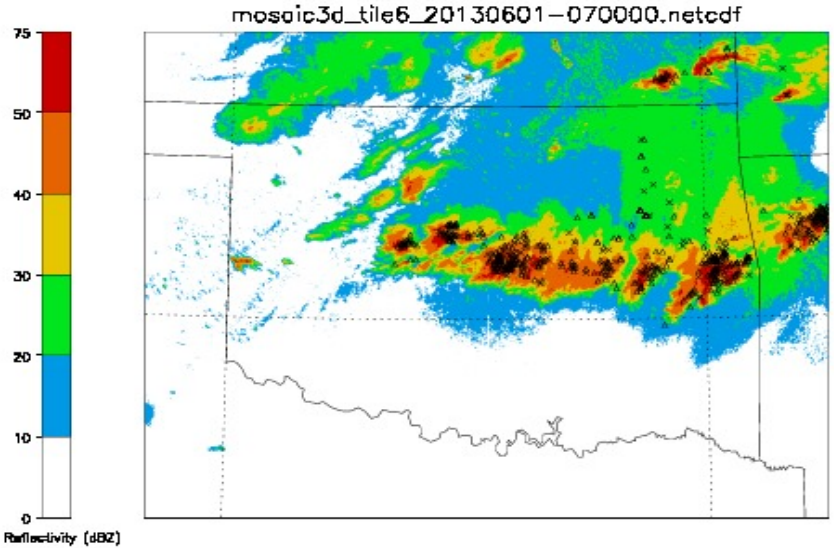
mosaic3d_tile6_20130601-070000.netcdf
75
50
40
30
20
10
0
Reflectivity (dBZ)

B

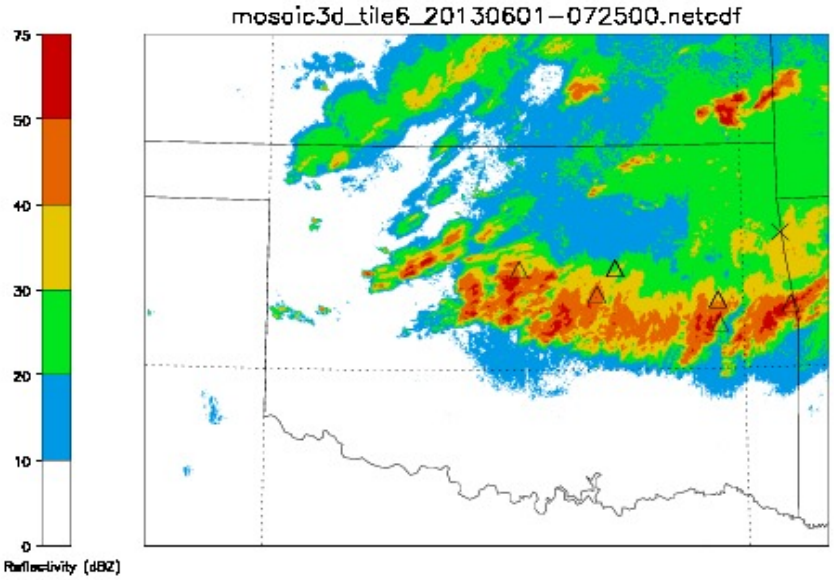
mosaic3d_tile6_20130601-072500.netcdf
75
50
40
30
20
10
0
Reflectivity (dBZ)

C

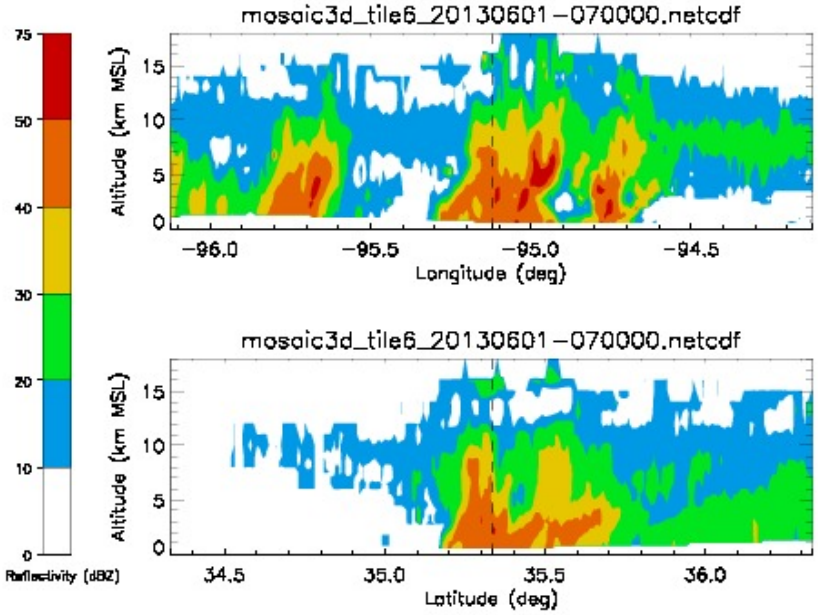

Figure 19. A) 1 June 2013 shows an hourly composite radar reflectivity and large CMC (>75 C km) discharges over OK (positive are X symbols and negative are triangle symbols). (B) represent the NLDN product for CMCs discharges. (C) composite radar reflectivity and negative CMC (>75 C km) discharges over OK. (D) represent vertical cross section of high reflectivity in one part of the storm. The black line represents the tropopause at 267.0 mb.